Наносистеми, наноматеріали, нанотехнології
Nanosystems, Nanomaterials, Nanotechnologies
2013, т. 11, № 3, сс. 605–617

PACS numbers: 62.80.+f, 81.05.Rm, 81.05.U-, 81.70.Cv, 82.45.Yz, 82.47.Uv, 84.60.Ve

Influence of Ultrasonic Treatment of Activated Carbon in Cavitation and Precavitation Regimes on Capacitive and Pseudocapacitive Energy Storage in Electrochemical Supercapacitors

B. Ya. Venhryn, I. I. Grygorchak, B. P. Bakhmatyuk, Yu. O. Kulyk*, and S. I. Mudry*

Lviv Polytechnic National University,
12 Bandera Str.,
79013 Lviv, Ukraine
**Ivan Franko National University of Lviv,*
8 Kyrylo and Mefodiy Str.,
79005 Lviv, Ukraine

Influence of ultrasonic treatment of activated carbon on the electric double layer in interface between the carbon and the 7.6 m KOH, 4 m KI, and 2 m ZnI_2 aqueous electrolyte solutions as well as on the working parameters of supercapacitors on their base is studied by means of precision porometry, small angle X-ray scattering, cyclic voltamperometry, electrochemical impedance spectroscopy, and computer simulation methods. As shown, the ultrasonic treatment at precavitation regimes causes the significant (more than by 200 times) increase of density of states at the Fermi level that is the reason not only quantitative but also qualitative changes in farad–volt dependences. At the same time, an acoustic cavitation field unblocks the Helmholtz capacitance due to large decrease of volume-charge-region resistance. Using these data, we propose the new electrochemical system of functional-hybrid supercapacitor with specific capacitance 1100 F/g and specific energy 49 W·h/kg.

За допомогою прецизійної порометрії, малокутового Рентґенового розсіяння, циклічної вольтамперометрії, електрохемічної імпедансної спектроскопії та комп'ютерного моделювання досліджено вплив ультразвукового оброблення активованого вугілля на параметри подвійного електричного шару межі поділу його з водними розчинами електролітів 7,6 m KOH, 4 m KI і 2 m ZnI_2 та експлуатаційні характеристики суперконденсаторів на їх основі. Показано, що ультразвукове оброблення докавітаційними режимами призводить до значного (більше ніж у 200 разів) збільшення густини станів на рівні Фермі, що призводить не тільки до

кількісних, але і до якісних змін вольт-фарадних залежностей. В той же час вплив поля акустичної кавітації деблокує Гельмгольцову місткість за рахунок сильного зменшення опору области просторового заряду в твердому тілі. На основі одержаних даних розроблено електрохемічну систему гібридного суперконденсатора з питомою місткістю у 1100 Ф/г і питомою енергією у 49 Вт·год/кг.

С помощью прецизионной порометрии, малоуглового рентгеновского рассеяния, циклической вольтамперометрии, электрохимической импедансной спектроскопии и компьютерного моделирования исследовано влияние ультразвуковой обработки активированного угля на параметры двойного электрического слоя границы его раздела с водными растворами электролитов 7,6 m KOH, 4 m KI и 2 m ZnI_2 и эксплуатационные характеристики суперконденсаторов на их основе. Показано, что ультразвуковая обработка докавитационными режимами приводит к существенному (больше чем в 200 раз) увеличению плотности состояний на уровне Ферми, что вызывает не только количественные, но и качественные изменения вольт-фарадных зависимостей. В то же время влияние поля акустической кавитации деблокирует гельмгольцевскую ёмкость за счёт сильного уменьшения сопротивления области пространственного заряда в твёрдом теле. На основании полученных данных разработана электрохимическая система гибридного суперконденсатора с удельной ёмкостью 1100 Ф/г и удельной энергией 49 Вт·ч/кг.

Key words: ultrasonic treatment, pseudocapacitance, electric double layer, Nyquist plots, hybrid supercapacitor.

(Received 2 February, 2012; in final version, 7 August, 2012)

1. INTRODUCTION

Supercapacitors, in which the high reversible electrochemical charge-discharge processes occur, have in few times larger specific power and in few hundred times the number of cycles than chemical accumulators, although their specific energy is lower. Supercapacitors, depending on mechanism of storage processes, can be divided into two groups. First of them consists of so called electrical double layer capacitors (EDLC), which capacitance is maintained by electric double layer (EDL) that is formed at the boundary between huge surface area (1000–3000 m^2/g) of blocking electrode with electrolyte. According to [1], the maximum differential EDLC capacitance is not higher than 25–30 $\mu F/cm^2$. The special kind of electrochemical supercapacitors, which capacitance is maintained by Faraday redox processes of definite nature belongs to the second group [1]. Up to now, there is no reasoned justifications concerning to neglecting the some components of capacitance for known kinds of activated carbon. Moreover, it is the most probably that, due to just Faraday pseudocapacitance, there is inconsistency of

experimentally determined values of specific capacitances (see, for instance, [2, 3]) with theoretically estimated value, which even out of BDM (Bockris, Devanathan and Müller) model [4] for electric double layer cannot exceed the value ≅ 140–150 F/g. It is conditioned by the fact that, at limited development of surface, the differential capacitance of known kinds of carbon and electrolyte systems due to the increase of the Thomas–Fermi screening length in electrode material does not exceed 15–17 $\mu F/cm^2$ [5], and electrochemical accessibility of surface is equal to ≅ 30% [6].

Obtained specific values of pseudocapacitance per unit electrode area are higher by one order then corresponding values of the EDLC typical electrostatic capacitances. According to [7], it is suggested to increase an energy density up to value 88.5 Wh/kg for supercapacitors on the carbon-based materials with ability to ion electrochemical intercalation. On the reason that total energy resource prevails $E = E_c N$ (E_c is mean energy of one 'charge–discharge' cycle, N—their number) of electrochemical capacitors comparing to chemical accumulators, at present time an intense studies, aimed on the decrease of both electrostatic and pseudocapacity contributions are carried out. In the first case, the works relate with searching of new kinds of carbon aerogels and nanotubes are dominant [8–10], whereas in the second one the tremendous efforts are aimed on the substitution of very expensive ruthenium and iridium oxides, maintaining the specific redox-capacitances up to 900 F/g [11, 12]. Success of this way is not as impressive as was expected, but nevertheless, some promising results were obtained. In particularly, the possibility to use the abilities of anions Cl^-, Br^- to specific absorption in order to increase the specific capacitive characteristics of carbon electrode is shown in [13]. Early in [14], we have established the reverse charge of activated carbon to 2000 F/g, based on intercalation process of anions I^- at electrode potential values not higher than at electrode potentials, no attaining both the potential of iodine extraction in free state of I_3^- potential formation. Our studying of interrelation between porous structure, electronic properties of nanoporous carbon and capacitance of carbon–electrolyte interface shown that contribution of pseudocapacitive charge storage in electric double layer more depends on Fermi level position in carbon materials and less depends on ion thermodynamic parameters in electrolyte solution [14]. Theoretical analysis of processes, which occur at interface between nanoporous carbon and electrolyte, carried out in this work, enabled us to hallmark for intercalative nature appearance as formation of discontinuous series of valence stable intercalate phases.

The measured data on farad–volt dependences for different electrolytes (KOH, KBr, CsBr, KI) show their sharp asymmetry in cathode and anode regions because of formation of great pseudocapacitance up

to 2000 F/g in anode region (KI); they also show very small capacitive charge accumulation (no more than 5.4 F/g) in anode region (KOH). In the former case, this asymmetry is mainly related with shunting of Helmholtz's layer capacitance by great faradaic capacitance (pseudocapacitance); in the latter case, this is connected with sharp expansion of spatial charge region in a solid. The formation of great capacitance (225 F/g) for the Cs^+ ion in negative region and superhigh pseudocapacitance (2000 F/g) for the I^- ion is caused by the ability of these ions to intercalate nanopores of activated carbon ($d \leq 4.4$ Å) that requires minimal value of chemical potential and hydration energy of the ion in a solution. The influence of electronic structure on the charge accumulation in EDL is discussed in this work.

At the same time, it follows from measurements of farad–volt plots in various electrolyte solutions (KOH, KBr, CsBr, and KI) that essential anisotropy exists in both cathode and anode region [14]. It is shown that shunting of Helmholtz layer capacitance by one of volume charge region in solid is the reason of low specific capacitance at negative polarisation of activated carbon.

Therefore, today's problems, which restrict the effectiveness of capacitive and pseudocapacitive energy storage in supercapacitors, are as follow:

limiting influence of depleted capacitance of volume charge region C_{SC} of activated carbon at negative electrode polarization in alkaline electrolyte; it is clear that unblocking of Helmholtz capacitance is promoted by increasing of C_{SC}, which, in turn, is proportional to density of states of delocalized charge carries at Fermi level $D(E_F)$ in accordance with well-known relation [15]:

$$C_{SC} = e_0 \sqrt{\varepsilon_{SC} \varepsilon_0 D\left(E_F\right)}; \quad (1)$$

absence of effective and suitable controlling methods by energy topology of electron states (*i.e.* the controlled variability of Fermi level position) for any chosen activated carbon in order to increase the specific pseudocapacitance, especially at large current load in case of positive polarization.

Generally, using of the high conductive forms of carbon (for instance, nanotubes) can help to avoid these problems. Unfortunately, today high cost and problem on maintaining of hydrophility do not permit to apply this method. On that reason, searching of new technology solutions in this field is the main aim of this work.

2. EXPERIMENTAL

Activated carbons of various origin, obtained by means of activated carbonization of birch wood (BW), cherry fruit stones (CFS) and sty-

rene-benzene copolymer (SBC) were chosen as materials under investigation. Their porous structure has been determined by means of both precision porometry method and small angle X-ray scattering [16] with using of ASAP 2000 M equipment and DRON-3 X-ray diffractometer. Ultrasonic treatment has been carried out in glass Pyrex ampoule, in which the activated carbon, dispersed in aqueous medium was placed. Ampoule was fixed in centre of piezoceramic sphere of 70 mm diameter. Ultrasonic irradiation has been performed at frequency of 22 kHz. One of the main parameters of ultrasonic treatment was irradiation duration, which in our experiments was chosen to be 5–14 hours for precavitation regime and only 5–15 minutes for cavitation one.

Electrochemical measurements have been carried out, according to two- and three-electrode setups with chlorine–silver reference electrode. Materials under investigation with binder (5% of polyvinilidenefluoride) have been forced on nickel or steel set of 0.5 cm^2 area. Aqueous solutions 7.6 m KOH, 4 m KI and 2 m ZnI_2 were chosen as electrolytes. Electrode potentials E have been recounted in reference to standard hydrogen reference electrode. Extraction potentials E and chemical potentials of ions μ_s have been calculated, according to well-known relations [17]:

$$E = E_0 + \frac{RT}{nF} \ln\left(\frac{a_{\text{oxid}}}{a_{\text{red}}}\right), \tag{2}$$

$$\mu_s = \mu_s^{\text{stand}} + RT \ln\left(a_s\right), \tag{3}$$

where a_{oxid}, a_{red}, a_s—activities of ions in solution. Energy levels have been determined in eV according to absolute energy scale.

Impedance spectra (in frequency region $5 \cdot 10^{-3}$–10^5 Hz and 5 mV of amplitude) in potentiostatic conditions, cyclic voltammograms and galvanostatic charge–discharge cycles were recorded with use of measuring equipment 'Autolab' ('Eco Chemie', Holland), attached with software FRA-2 and GPES. Obtained impedance data have been simulated to accordance with electric equivalent circuits in medium of program pack ZView 2.3 (Scribner Associates). Capacitance values for plotting farad–volt dependences have been determined from virtual value of hodograph impedance at frequency $5 \cdot 10^{-3}$ Hz with accuracy 2–8% (Kramers–Kronig test was performed within 10^{-6}–10^{-5} interval) according to well-known formula: $C = (j2\pi f Z'')^{-1}$.

3. RESULTS AND DISCUSSION

As shown in Fig. 1, where the size distribution functions for materials under investigation are represented, all they reveal the optimal [18] pore diameter d distribution function for capacitive charge storage

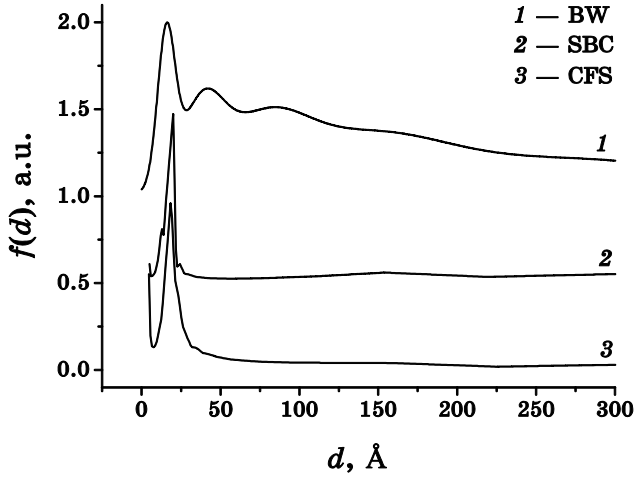

Fig. 1. Pore distribution function versus diameter.

TABLE 1. Porometric characteristics of investigated carbons.

Material	Specific surface area, m^2/g		
	$d \le 4.4$ Å	$4.4 < d < 19$ Å	$d > 19$ Å
SBC	576	332	120
CFS	448	498	181
BW	134	264	69

with maximum in vicinity $d = 2$ nm and similar behaviour within the micro- and mesopores' region. However, a total areas of all porous surfaces, in which the formation of compact screened electric double layer is problematic ($d \le 4.4$ Å), are notably different (Table 1).

Studies of ultrasonic treatment influence on specific capacitance reveal the dependence of parameter under consideration from both irradiation condition and kind of activated carbon. It is noteworthy that cavitation regimes that were investigated here (for which the duration was not longer than 15 min on the reason of no admission of activated carbon dispersing by cavitation streams) change the value of specific capacitance less remarkably not only to its increase (for BW) but to decrease too (for SBC). The difference between those materials is, first of all, in their electron structure, characterized by different positions of the Fermi level, which determines the value of electrochemical potential $\tilde{\mu}$, measured by means of experimental method [19]. These values are found to be $\tilde{\mu} = -0.42$ V, (BW) and $\tilde{\mu} = -4.08$ V (SBC).

But, as was revealed, the cavitation regimes decrease the frequency dependence of capacitance within the frequency range 1–50 Hz (Fig.

2). It means that such materials maintain higher power at current loads corresponding to that frequency range. Moreover, they are promising for development of carbon supercapacitors for circuits with alternating current.

In order to understand the physical nature of observed phenomena, let us consider the impedance spectroscopy data. First of all, it should be noted that Nyquist plots for all regimes of cavitation modification have the typical shape (Fig. 3), which indicates the state of distribution ('deformability') of capacitance. This fact as well as necessary to take into account the capacitance of volume charge region (VCR) at

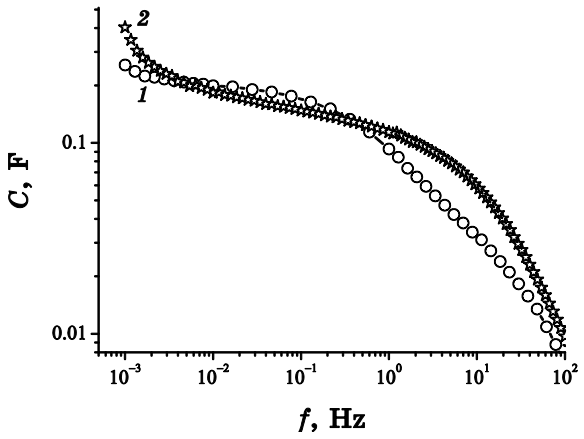

Fig. 2. Capacitance dependence versus frequency at negative polarization for BW before (*1*) and upon ultrasonic treatment in cavitation regimes (*2*).

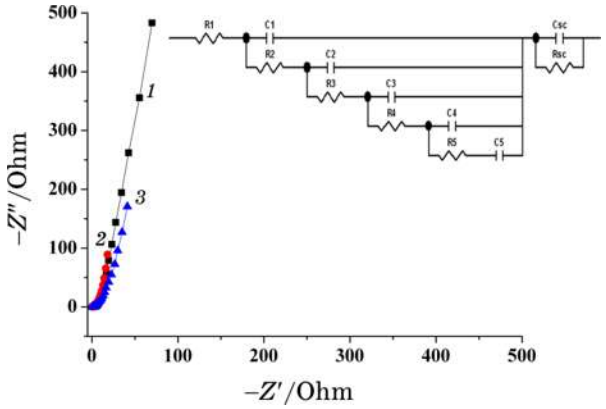

Fig. 3. Nyquist plot behaviour for initial carbon (*1*) and upon cavitation ultrasonic irradiation in 50 ml H_2O during 5 min (*2*) and 20 min (*3*). Insert—equivalent electric circuit.

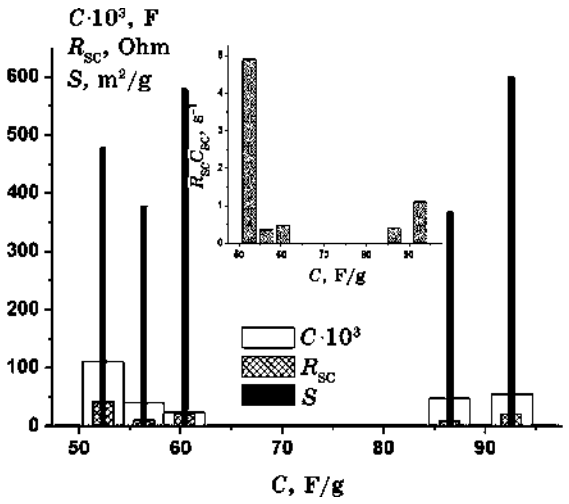

Fig. 4. Interrelation between parameters of electric double layer and values of specific capacitance at galvanostatic discharge.

formulation of adequate impedance model need to use de Levie model [20], modified by daisy chains of parallel $R_{SC}C_{SC}$-link of chain, as it is shown in insert to Fig. 3. Here, R_{SC} and C_{SC} are resistivity and capacitance of VCR, respectively. The results of computer parametric identification are displayed as bar graphs in Fig. 4, where C_H marks the capacitance of Helmholtz layer.

Above all, it can be seen that ultrasonic irradiation promotes to C_{SC} decrease (non-monotonic with increasing both t and C), that in compliance with (1) is the evidence of density of states at Fermi level decrease. The direct confirmation of this was obtained by our results on electron emission X-ray spectroscopy. Hence, the spectrum of valence band for initial activated carbon has a two-shoulder shape with significant decrease of intensity at attaining of bonding energy to Fermi level. The intensity at Fermi level, which is proportional to electron density, equals $I(E_F) = 13630$ a.u. After ultrasonic irradiation, the shape of valence band no changes significantly, but visible intensity decrease at Fermi level to $I(E_F) = 9300$ a.u. is observed.

At the same time, it is shown that ultrasonic irradiation leads also to R_{SC} decrease with nonmonotonic behaviour, no adequate to nonmonotonic behaviour of C_{SC}, that no correlates with decrease of $D(E_F)$. Thus, C_{SC} and R_{SC} decrease no find their adequate representation in decrease of measured specific discharge capacitance C in 'charge–discharge' galvanostatic cycles (Fig. 4). This allows asserting that the time constant $R_{SC}C_{SC}$-link (inset to Fig. 3) should be chosen as decisive factor for the C value, which in fact represents:

a) shunting of C_{SC} by resistance of VCR, *i.e.* in this case, R_{SC} reveals the

fact that effective unblocking of Helmholtz capacitance is observed when the time of plate charging C_{SC} is higher than period of its oscillations;
b) symmetrisation of voltage–current characteristic for regions of cathode and anode polarisation.

Thus, the values of measured capacitance correlate in nontrivial way with parameters of EDL. The data obtained for materials under investigation allow us to state that, in hierarchy aspect for the equal values of active surface areas, the most effective unblocking of Helmholtz capacitance can be reached when the resistance of VCR is low (see inset to Fig. 3).

Concerning to physical nature of observed changes, it includes, at least, two aspects:
a) we deal with untypical for carbon-graphite materials, but well known for semiconductors [21] phenomenon of admixture redistribution, stimulated by ultrasonic radiation that results in modification of impurity energetic topology;
b) strong dependence of mobility and, may be, philinity on fractal structure.

The direct confirmation of the first of them is the data of quantitative and qualitative analysis of carbon materials before and after ultrasonic treatment in different regimes by means of scanning electron microscope 'JEOL'. Data on distribution of chemical elements, which materials under investigation consist of, are listed in Table 2. In other words, it is possible to control the surface electron states created by impurities as well as intrinsic defects by means of ultrasonic irradiation.

The aspect of physical nature of observed changes means that dominating contribution to the R_{SC} value makes not concentration of delocalized electrons, but mobility, which should be related to kind of fractal structure. Comparison of C_H and S (Fig. 4) is a good evidence for this.

TABLE 2. Distribution of chemical elements before and after ultrasonic treatment of carbon material.

Element	Weight, %		Atomic, %	
	initial	after ultrasonic treatment	initial	after ultrasonic treatment
C	91.5	95.0	94.3	96.3
O	6.5	4.7	5.0	3.6
Mg	0.2	—	0.1	—
K	1.2	—	0.4	—
Ca	0.6	0.3	0.2	0.1
Total	100.00	100.00	100.00	100.00

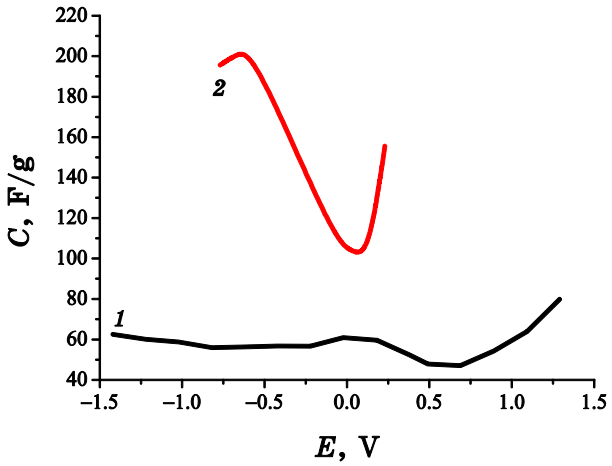

Fig. 5. Farad–volt dependences in 7.6 m KOH for initial activated carbon (*1*) and after precavitation ultrasonic treatment (*2*).

The question arises whether the mechanism of precavitation influence on storage properties of activated carbon is adequate. In order to answer this question, the attention should be paid to the first fact that C_{spec} values represent evidently the notable pseudocapacitive contribution at negative polarization of nature origin carbon materials. Secondly, the increase of maximum capacitance in 7.6 m KOH both in cathode and anode region and change of farad–volt curve behaviour after ultrasonic precavitation treatment show that interval, where the capacitance decreases with increasing of anode polarization potential (Fig. 5), that is the characteristic of initial material (curve *1*), and its increasing from minimum value 155 F/g at 0.1 V to 166 F/g at 0.3 V (curve *2*) does not exist already. Minimum in C–E dependence at 0.1 V corresponds to zero charge as it is commonly observed for neutral and acid electrolyte. Limitation of further charging corresponds of EDL and is related to attaining of discharge potential OH^- ion, which forms the Helmholtz layer within that range of potential values.

Using relation (1) for experimentally obtained values of differential capacitance at zero charge, value of potential φ_{zc} and value of $C_H = 20$ μF/cm^2, $\varepsilon = 3.3$ [22], the differential capacitance $C_{SC} = 44$ μF/cm^2 and density of states at the Fermi level $D(E_F) = 4.1 \cdot 10^{22}$ cm^{-3}·eV^{-1} have been calculated. The last value is by 200 times higher than $D(E_F)$ for initial activated carbon that, contrary to cavitation treatment, just maintains in that case the unblocking of Helmholtz layer capacitance C_H.

Special attention is being paid to results on anode polarization of investigated carbons in ZnI_2 (Fig. 6). Obtained colossal value of C_{spec} indicates preferred and decisive contribution of pseudocapacitance. As follows from literature, the ability of I^- to specific absorption on the sur-

face of platinum and mercury as well as property of positive carbons to absorb the anions from solutions takes place [13, 23]. For our case, taking into account the large number of nonelectrolytic pores (Table 1), the intercalative nature of pseudocapacitance, which was proved by us both in theoretical and experimental way, should be expected to be pronounced. Besides, in $-Z'' - Z'$ plots for ACM electrodes in 2 m KI at mean frequencies, as it should be expected, the Faraday loop can be selected. The reversibility of processes for ACM electrode in 2 m ZnI_2 aqueous solutions (Fig. 7) is illustrated in cyclic voltage–current plots, recorded according to three-electrode circuit at tenth cycle.

The possibility of practical application of large reversible I^- intercalative pseudocapacitance of ACM porous structure has been investigated in 2 m ZnI_2 with zinc-metallic antielectrode and reference electrode. Thermodynamic parameters of I^- ion in that electrolyte are in fact the same as for 4 m KI. At measuring, the following electrochemical system was used:

$$\mathrm{ACM}\left|2m\mathrm{ZnI_2}\right|\mathrm{Zn}\,, \qquad (4)$$

which had the voltage of opened circuit $E_{oc} = 1.10$ V. Minimum in cyclic volt-amperogram recorded to three-electrode circuit (Fig. 7) corresponds to maximum cathode (discharge) current. The discharge capacitance calculated at those conditions in 2 m ZnI_2 was found to be 1150 F/g.

For electrode charging according with two-electrode setup, the anode polarisation in potentiostatic conditions at 1.245 V was applied. Galvanostatic discharge with current $I = 0.5$ A/g before charged ACM runs at mean discharge current 1.14 V and provides discharge capacitance 1100 F/g (43 mAh/g). Specific energy equals to $W = 49$ Wh/kg.

4. CONCLUSIONS

1. Precavitation ultrasonic treatment of activated carbon results in more than two orders increase of density of states at Fermi level that is decisive factor in colossal increasing of specific capacitance, mainly due to unblocking of Helmholtz capacitance by volume charge region capacitance in carbon. Value of galvanostatic discharge capacitance, which equals to 260 F/g in 7.6 m KOH with current density 5 A/g suggests proposed technology promising for EDLC.

2. The reason of working characteristics improving at cavitation ultrasonic irradiation is the remarkable reduction of time constant of $R_{SC}C_{SC}$-chain generally and R_{SC} in particular. The changes of double electric layer parameters is directly related with fractal dimension, which, in turn, increases the percolation mobility of charge carries at given parameters of ultrasonic radiation.

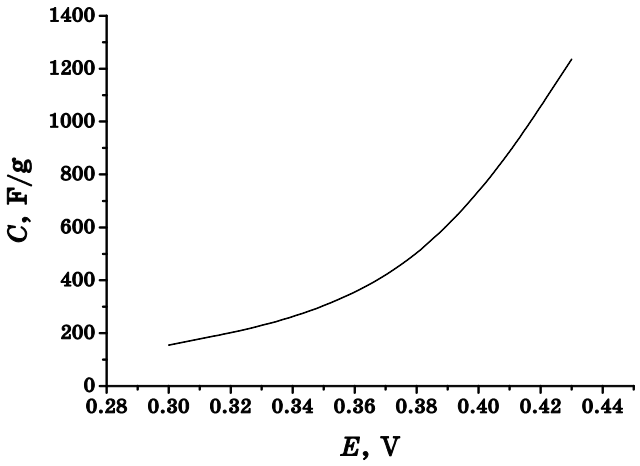

Fig. 6. Farad–volt dependence for ACM in 4 m KI within the positive potential region.

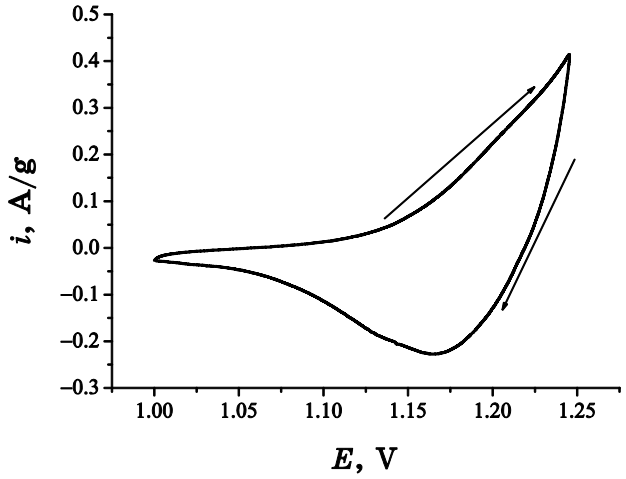

Fig. 7. Cyclic voltage–current plot recorded with scanning rate $\upsilon_p = 2 \cdot 10^{-4}$ V/s of ACM electrode in 2 m ZnI_2.

3. The influence of cavitation ultrasonic irradiation on pseudocapacitive energy storage leads to decrease of capacitance frequency dependence and increase of faraday loop.

REFERENCES

1. B. E. Conway, *Electrochemical Supercapacitors* (New York: Plenum Publishing: 1999).

2. S. Dietz and V. Nquen, *Proc. 10-th International Seminar on Double Layer Capacitor and Similar Energy Storage Devices (Deerfield Beach, USA, 2000)*, p. 7.
3. H. Shi, *Electrochim. Acta*, **41**, No. 10: 1633 (1996).
4. J. O'M. Bockris, M. A. V. Devanathan, and K. Muller, *Proc. R. Soc.*, **A274**, No. 1356: 55 (1963).
5. G. Gryglewicz, J. Machnikowski, E. Lorenc-Grabowska, G. Lota, and E. Fraçkowiak, *Electrochim. Acta*, **50**, No. 5: 1197 (2005).
6. A. D. Little, *Proc. 4-th International Seminar on Double Layer Capacitor and Similar Energy Storage Devices (Deerfield Beach, USA, 1994)*, p. 32.
7. J. P. Zheng, *Proc. 14-th International Seminar on Double Layer Capacitors and Hybrid Energy Storage Devices (Deerfield Beach, USA, 2004)*, p. 142.
8. Y.-Z. Wei, B. Fang, S. Iwasa, and M. Kumagai, *J. Power Sources*, **141**, No. 2: 386 (2005).
9. B. Zhang, J. Liang, C. L. Xu, B. Q. Wei, D. B. Ruan, and D. H. Wu, *Mater. Lett.*, **51**, No. 6: 539 (2001).
10. K. H. An, K. K. Jeon, J. K. Heo, S. C. Lim, D. J. Bae, and Y. H. Lee, *J. Electrochem. Soc.*, **149**, No. 8: A1058 (2002).
11. J. P. Zheng and T. R. Jow, *J. Electrochem. Soc.*, **142**, No. 1: L6 (1995).
12. D. A. McKeown, P. L. Hagans, L. P. L. Carette, A. E. Russell, K. E. Swider, and D. R. Rolison, *J. Phys. Chem. B*, **103**, No. 23: 4825 (1999).
13. B. E. Conway, H. A. Andreas, and W. G. Pell, *Proc. 14-th International Seminar on Double Layer Capacitor and Hybrid Energy Storage Devices (Deerfield Beach, USA, 2004)*, p. 155.
14. B. P. Bakhmatyuk, B. Ya. Venhryn, I. I. Grygorchak, M. M. Micov, and Yu. O. Kulyk, *Electrochim. Acta*, **52**, No. 24: 6604 (2007).
15. H. Gerischer, *J. Phys. Chem.*, **89**, No. 20: 4249 (1985).
16. R. N. Kyutt, E. A. Smorgonskaya, S. K. Gordeev, A. B. Grechinskaya, and A. M. Danishevskiy, *Fizika Tverdogo Tela*, **41**, No. 8: 1484 (1999) (in Russian).
17. A. M. Sukhotin, *Handbook on Electrochemistry* (Leningrad: Khimiya: 1981) (in Russian).
18. B. E. Conway, *Proc. 3-rd International Seminar on Double Layer Capacitor and Similar Energy Storage Devices (Deerfield Beach, USA, 1993)*, p. 28.
19. Yu. Ya. Gurevich and Ju. B. Pleskov, *Photoelectrochemistry of Semiconductors* (Moscow: Nauka: 1983) (in Russian).
20. R. de Levie, *Advances in Electrochemistry and Electrochemical Engineering* (New York: Interscience: 1967), vol. **4**.
21. I. V. Ostrovskii, A. B. Nadtochiy, and A. A. Podolyan, *Fizika i Tekhnika Poluprovodnikov*, **36**, No. 4: 389 (2002) (in Russian).
22. S. Ergun, J. B. Yasinsky, and J. R. Townsend, *Carbon*, **5**, No. 4: 403 (1967).
23. A. N. Frumkin, *Potentials of a Zero Charge* (Moscow: Nauka: 1979) (in Russian).
24. J. V. Coe, *Chem. Phys. Lett.*, **229**, Nos. 1–2: 161 (1994).
25. M. D. Tissandier, K. A. Cowen, W. Y. Feng, E. Gundlach, M. H. Cohen, A. D. Earhart, J. V. Coe, and T. R. Tuttle, Jr., *J. Phys. Chem. A*, **102**, No. 40: 7787 (1998).